Transformation of molecular nitrogen to nonmolecular phases at megabar pressures by direct laser heating

M. J. Lipp, J. Park Klepeis, B. J. Baer, H. Cynn, W. J. Evans, V. Iota, and C.-S. Yoo
Lawrence Livermore National Laboratory, Livermore, California 94550, USA
(Received 1 December 2006; revised manuscript received 30 March 2007; published 19 July 2007)

Direct laser heating of molecular N_2 to above 1400 K at 120–130 GPa results in the formation of a reddish amorphous phase and a transparent crystalline solid above 2000 K. Raman and x-ray data confirm that the transparent phase is *cubic-gauche* nitrogen (cg-N), while the amorphous phase could be an extension of the already known η phase. The reddish color of the amorphous phase, however, might also indicate the presence of N═N bonds. The quenched amorphous phase is stable down to at least 70 GPa, analogous to cg-N. A chemophysical phase diagram is presented which emphasizes the difference between pressure- and temperature-induced transitions from molecular to nonmolecular solids, as found in other low *Z* systems.

DOI: 10.1103/PhysRevB.76.014113 PACS number(s): 62.50.+p, 61.50.Ks, 64.30.+t, 78.30.−j

Extended forms of simple low-*Z* materials are of fundamental importance in developing condensed matter theory[1,2] and novel materials with advanced mechanical, optical, and energetic properties.[3–5] These materials, however, are typically stabilized at formidable pressure-temperature conditions, thus imposing tremendous technical challenges that at present can only be realized in a diamond anvil cell (DAC). At a pressure of 100 GPa (or 1 Mbar) and a compression energy ($P\Delta V$) often exceeding 1 eV, localized electrons have acquired very high kinetic energy and can therefore mix strongly with valence and core electrons of their own or nearby molecules. Such core swelling and/or valence mixing can induce transformations from molecular to nonmolecular extended solids such as polymers and metals.[6] A competing pathway is provided by rapid electronic band broadening leading to an insulator-metal transition. Materials at high temperatures, on the other hand, often transform into open structures like bcc because of the large increase in entropy and eventually ionize, dissociate, or even decompose. Combining the effects of extreme pressure and temperature (or *megabar chemistry*), one can probe the balance between pressure-induced electron delocalization ($P\Delta V$) and temperature-induced electron ionization ($T\Delta S$), as is reflected in crystal structures, phase boundaries, and stabilities.

The behavior of nitrogen presents a prime example. It displays a large number of polymorphs, both molecular and nonmolecular,[7,8] with widely different intermolecular interactions, crystal structures, and chemical bonds. Among those, the prediction and discovery of cubic-*gauche* nitrogen (cg-N) are the most celebrated recent example,[1,9] where molecular nitrogen in the ζ phase transforms to a nonmolecular extended solid, with the atoms arranged in a puckered layer structure. Because cg-N is built by strong N—N covalent bonds, replacing substantially weaker intermolecular interactions in ζ-N_2, the material strength of cg-N is greatly enhanced to support large lattice strains and exhibits a large activation barrier toward the reverse transformation. In fact, cg-N is predicted to be metastable even at ambient conditions.[10] Furthermore, the theory[1] predicts that cg-N contains a high energy density, stimulating the experimental efforts to synthesize it by chemical methods.[11]

High-pressure synthesis of cg-N poses great experimental challenges. While previous theoretical calculations[1] predicted that transformation conditions should be in reach at a pressure of 50±15 GPa at room temperature, the first experimental claim reported a pressure of at least 110 GPa and a temperature of 2000 K.[9] In fact, the discovery appeared to require several key modifications to the traditional DAC geometry, among them the deliberate placement of thin sheets of infrared laser (1064 nm) absorbing materials covering the whole sample chamber to generate the necessary temperatures, as well as the use of nonmetallic c-BN gasket inserts.[9] While apparently necessary in achieving the transformation conditions, the introduction of boron, TiN, or platinum has, nevertheless, cast some doubts on the experimental results, especially with regard to the possibility of highly exothermic reactions between the absorber plates and the nitrogen sample itself as observed by others previously.[12–14] For example, the onset of the reaction between boron and nitrogen under a pressure of 10 GPa requires 1800 K, very similar to the temperatures required for the synthesis of polymeric nitrogen.[12] Moreover, the synthesis of other nitrides, such as PtN_2 or IrN_2, from their elemental constituents also requires threshold pressures and temperatures in excess of about 50 GPa and 2000 K.[13,14] For PtN_2, one of the ensuing sharp Raman lines is actually observed in close proximity to the spectral position of the previously reported Raman line of cg-nitrogen. The authors of Ref. 9 provide angle dispersive x-ray scattering data as additional support for their claim, but even those results have recently been questioned,[15] and attempts to laser heat nitrogen in sample configurations similar to those in Ref. 9 with absorbers and gasket inserts have failed.[15]

We therefore attempted *direct* laser heating of pure nitrogen in the ζ-N_2 phase at 120–130 GPa in a traditional DAC geometry and found that it leads to the formation of two extended forms of nitrogen: reddish amorphous nitrogen and transparent crystalline nitrogen analogous to cg-N reported previously, as shown in Figs. 1 and 2. The reddish amorphous phase could be different from all other phases of nitrogen reported to date or it could be an extension of the previously observed η phase. Its existence is important to understand the subtle difference between the pressure- and temperature-induced changes that lead to different forms of

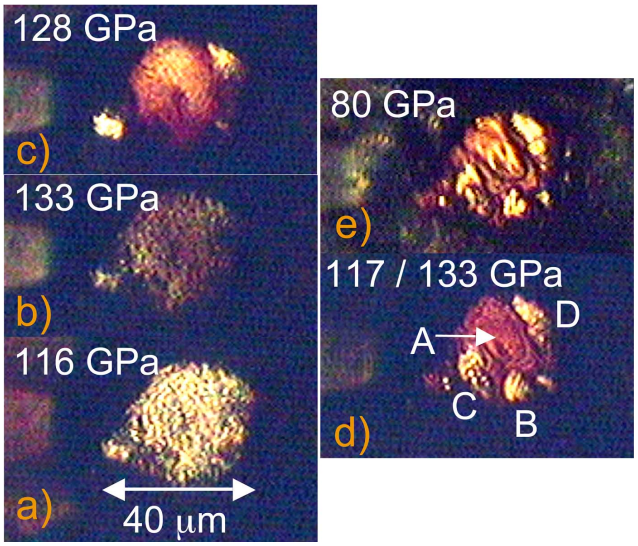

FIG. 1. (Color online) Microphotographic images of nitrogen phases in the first sample. All images were taken at room temperature. (a) Sample at 116 GPa; the sample is still transparent. (b) At 133 GPa, the sample has begun to darken considerably. (c) After the first laser heating to 1400 K. Raman spectroscopy still sees the molecular signature of the ζ phase (see Fig. 3, curve a). (d) After the second laser heating, the sample consists of several phases: reddish amorphous nitrogen at location A and single-bonded cg-N at locations B, C, and D. The sample sustains large pressure gradients (117 GPa at A and 133 GPa at B–D). (e) The sample after decompression to 80 GPa.

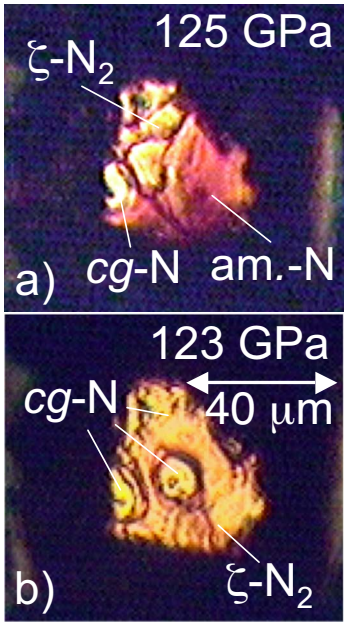

FIG. 2. (Color online) Microphotographic images of nitrogen phases in the second sample after the second heating to 2000 K. (a) The sample consists of several phases: reddish amorphous nitrogen (called am.-N), the single-bonded cg-N at the left edge, and the remaining ζ-N_2. (b) A third heating transformed even more of the sample to cg-N in the center and at the top, while the reddish amorphous phase has reverted back to molecular ζ-N_2. The slightly reddish color indicates that the back-transformation was not complete.

the extended phases observed and/or predicted to date.

For the experiments, we employed membrane-driven DACs designed and fabricated at LLNL, equipped with diamond anvils of 100 μm flats beveled out to a diameter of 300 μm at an angle of 8.5°. Ultrahigh purity nitrogen gas (99.999%) was condensed into a small sample chamber (~50 μm in diameter and ~25 μm thick) in a Re gasket in a cryogenic gas loading vessel. Pressures were measured by ruby luminescence up to 100 GPa, above by the diamond phonon line[16] for Raman studies, or by the tungsten equation of state[17] for x-ray studies. Heating was performed by focusing the 1053 nm radiation of two YLF lasers (~60 W) simultaneously onto the samples without use of any special laser irradiation absorbing agents. Temperatures were either measured by the spectroradiometric method or estimated.

Angle-dispersive x-ray diffraction images were obtained at the microdiffraction beamline 16IDB of the High Pressure Collaborative Access Team (HPCAT) at the Advanced Photon Source (APS). The recorded two-dimensional diffraction images were then integrated to produce the x-ray diffraction patterns using the FIT2D program and analyzed with the XRDA and GSAS software.

Nitrogen transforms into the ζ phase at 70 GPa and develops a brownish color [Figs. 1(a) and 1(b)] above 125–130 GPa, indicating the first changes on the way from the ζ to the η phase. Coherent anti-Stokes Raman spectroscopy (CARS) experiments on the sample (λ_1=532 nm, λ_2=608 nm) at 133 GPa indicated that the optical absorption gap had decreased into the visible region to about 2.62 eV (λ_{AS}=473 nm or 2.62 eV) since the anti-Stokes radiation of the CARS experiments was almost completely absorbed (reduction by more than a factor 10 compared to the intensity received at 120 GPa). This moment was therefore chosen to initiate laser heating in the hope that the tail of the optical absorption would extend out to 1053 nm (1.178 eV) and facilitate coupling between sample and laser radiation without an absorber plate. Figure 1 shows images of the first sample from several stages of the experiment: Panels (a) and (b) show the gradual darkening, (c) the sample after the first heating to 1400 K, (d) the formation of transparent and dark-red regions after the second heating, and (e) the sample after pressure release to 80 GPa shortly before gasket failure. Sample 2 went through the same stages with the same features except that after the second heating some molecular N_2 was still observed [Fig. 2(a)] and that a third heating converted the amorphous phase back to molecular N_2.

Both samples—one at 127 GPa and the other at 133 GPa—were heated first to 1400 K. We found a small pressure decrease (~2–5 GPa) and a color change to more reddish-yellowish, but the Raman spectrum was still characteristic of the ζ phase [Figs. 1(c) and 3, curve a]. Further heating of the samples to higher temperatures was challenging and required the full power of the laser heating system (on the order of 60 W), which even then led to a few bright flashes only. They appeared to correlate with the formation of the transparent regions [see Fig. 1(d)]. We estimated the peak temperature of the flashes to be at least 2000 K or

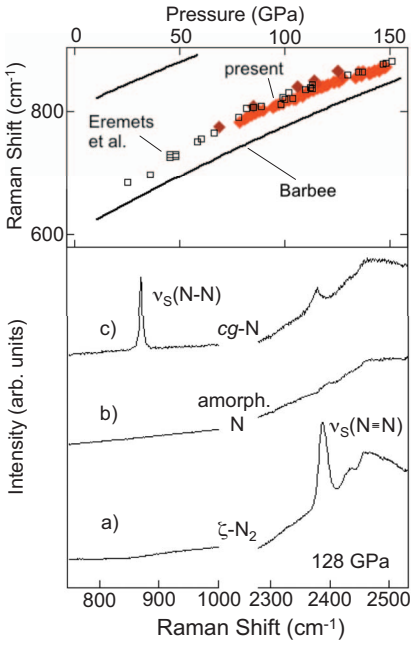

FIG. 3. (Color online) Raman spectra taken from quenched nitrogen after laser heating at 128 GPa. Bottom panel: (a) Untransformed ζ-N_2, (b) amorphous red phase as shown in Fig. 1(d) or 2(a) and 2(c) cg-N as recorded from the bright locations in Fig. 1(d) or 1(e) and Fig. 2(b). Top panel: Pressure shift of the Raman peak of the N—N bond. Red symbols represent current data, the black lines the calculations (Ref. 10) and the hollow squares the previous measurements (Ref. 9).

higher. The quenched samples showed that two phases were formed from the ζ phase [Figs. 1(d) and 2(a)]: dark reddish amorphous nitrogen with virtually no Raman features (Fig. 3, curve b) and the transparent crystalline phase (cg-N) exhibiting a sharp vibron at 865 cm^{-1} (Fig. 3, curve c). Note that the appearance of the 865 cm^{-1} band correlates with the disappearance of the N_2 vibron at 2390 cm^{-1}, clearly indicating the formation of an extended solid with N—N single bonds. No further change of the transparent cg-N phase could be induced in subsequent heating attempts once it was formed; however, the reddish amorphous phase could be transformed further to either cg-N or back to the ζ phase in the second sample [see Fig. 2(b)]. This indicates that the amorphous phase forms at somewhat lower temperatures than cg-N, presumably between 1400 and 2000 K.

Our observations during laser heating are similar to the ones made by Eremets *et al.*[9] in that a darkening of the sample was observed after heating to 1400 K, accompanied by a pressure drop but no significant change in the Raman spectrum of the molecular nitrogen. In Ref. 9, further heating to 1700 K produced even further darkening, with a significant decrease of the molecular vibron. With heating beyond 2000 K, the authors of Ref. 9 observed that the molecular Raman signatures in the lattice and vibron region all but vanished while a ring around the absorber plate appeared, which was attributed to melting and, instead of further darkening with even higher heat, the sample became transparent (albeit not visible in Ref. 9 due to the absorber plate). In our case, the sample coupled to the pump radiation only in some locations—mostly close to the edges of the gasket—and produced flashes that were estimated to be higher in temperature than ~2000 K, but the resulting dark red phase in the center and the large pockets of a transparent new phase are consistent with the observations in Ref. 9.

Both the reddish amorphous phase and the transparent cg-N phase were quenchable at least down to 70 GPa, where gasket failure occurred. The pressure dependence of the 865 cm^{-1} band is similar to that of the low-frequency Raman mode as calculated for the $I2_13$ structure (S.G. 199) and published previously[9,10] (Fig. 3, top panel). The Raman mode remains very sharp, full width at half maximum within ~6.5 cm^{-1}, over the entire range, so it can be used as an uncalibrated but very precise pressure sensor. On the other hand, the reddish amorphous phase [Figs. 1(d) and 2(a)] showed no Raman features (Fig. 3, curve b), kept its color over the entire pressure range [Fig. 1(e)], and induced strong photoluminescence from a 488 nm laser beam. Its distinctive reddish color could characterize it as being different from the amorphous nitrogen in the η phase[18–20] since we started out with a brownish and/or grayish sample color before heating and obtained a reddish color afterward, while the pressure remained almost unchanged. The distinctive red color of the amorphous phase observed here may represent the conversion of N≡N triple bonds to conjugated N=N double bonds. This conjecture could also explain the increase in color intensity with further heating, since the color of a system of conjugated double bonds (—N=N—N=N—) intensifies by increasing the number of double bonds.[21] Another explanation would be that simply more molecular nitrogen became converted to the amorphous phase. The presence of conjugated N=N bonds in the red amorphous phase then lowers the activation barrier for the formation of a singly bonded network structure and, thus, is likely a precursor to cg-N. The absence of this phase in previous experiments[9] might simply reflect the catalytic nature of the nitrogen conversion to cg-N on a surface of amorphous boron or TiN, thus bypassing this precursory state. In fact, we consider that such a strong kinetic effect may even retard, if not preclude, the formation of cg-N at ambient temperature even at 240 GPa. Further experiments are planned to determine the exact nature of the reddish amorphous phase. Several of our observations indicate that the reddish amorphous phase and the η phase are quite similar—on the other hand, the change to a red color after heating, with the pressure almost unchanged, points to some differences. The fact that the reddish phase can be converted back to molecular nitrogen eliminates impurities as the source of the reddish color.

Our x-ray diffraction data confirm the Raman result that the transparent phase is a cubic form of nitrogen. X-ray diffraction images (inset of Fig. 4) suggest moderate to strong preferred orientation. The pattern at 77 GPa contains additional traces of hcp Re and the pattern at 123 GPa shows the presence of the pressure marker tungsten. The intensity distribution, however, was found to be different from the previous report[9]: while we were able to extend the pattern to include the (321) peak at 2θ=25.83°, the (220) peak was either absent or barely visible in the patterns, and the (222) peak was also missing. The (*hkl*) extinction conditions are clearly matched to six cubic space groups: $I2_13$, $I23$, I-43m,

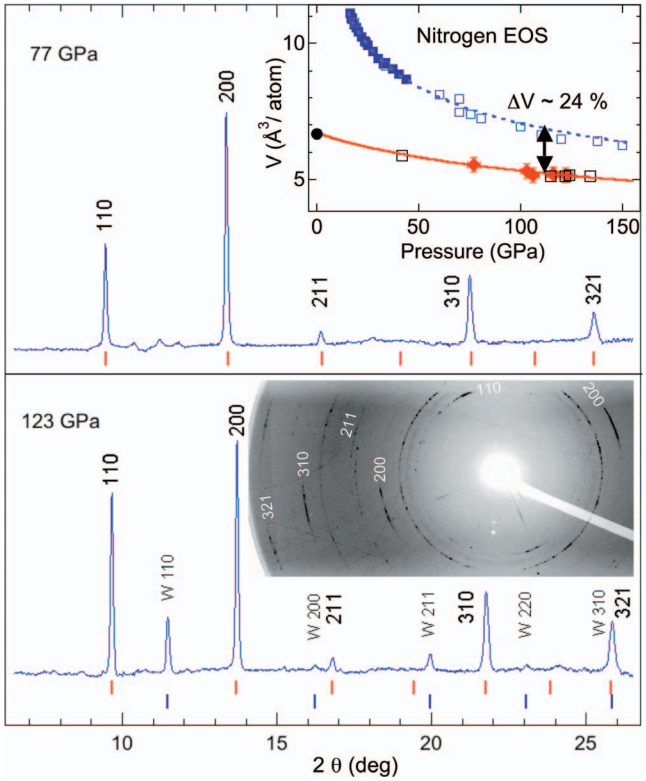

FIG. 4. (Color online) X-ray diffraction patterns of cg-N at 123 and 77 GPa after direct laser-heating. Beam size of 6×6 μm^2 and wavelength of 0.4125 Å. The 123 GPa pattern originates from the center close to the W pressure sensor [Fig. 2(b)]. The 2D image identifies the diffraction rings of cg-N. The 77 GPa pattern shows the diffraction at the center away from the W pressure sensor with small traces of ζ-N_2 and the Rhenium gasket. (Top inset) Atomic volume of cg-N vs pressure: Blue filled and hollow squares represent molecular N_2 (Refs. 22 and 23), the blue dashed line a Birch-Murnaghan fit. Red diamonds show the EOS data of cg-N from the present study, hollow black squares from previous data (Ref. 23). The black dot at $p=0$ signifies the theoretical prediction (Ref. 1).

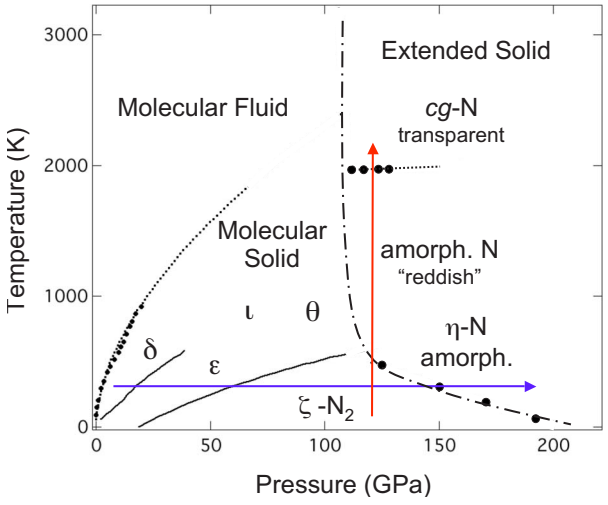

FIG. 5. (Color online) Conceptual phase/chemical transformation diagram of nitrogen illustrating the molecular to nonmolecular transformation at high pressures and temperatures. The transformation boundary (dot-dash line) is based on present and previous high-pressure data (Refs. 9, 18, 19, and 22–26). The melt curve (dotted line) represents a Simon-type extrapolation of previous melt data (small black dots) (Ref. 25). The molecular α, β, and γ phases at low pressures are not shown. Note that ζ-N_2 transforms into semiconducting amorphous η-N at low temperatures, yet becomes reddish amorphous nitrogen at medium and transparent cg-N at high temperatures. The strong curvature of the transformation boundary at lower temperatures signifies the strong kinetic effects associated with the molecular-to-nonmolecular transformation. Blue (compression) and red (heating) arrows represent experimental pathways.

$I432$, Im-3, or Im-3m. Density considerations require eight nitrogen atoms per unit cell. A calculation of the intensity distribution for the last three space groups does not produce a match. The first three space groups, however, allow the Wyckoff positions (8a or 8c) to vary. In principle, one could determine the x parameter from the intensity ratio of the (110) and (200) ring patterns despite the limited opening of the diamond anvil cell, which affects the diffraction peak intensities mainly at lower d spacing. The texture of the sample, however, renders the results for x and the bond lengths too speculative. For the 77 GPa pattern, the best match occurs again for space group $I2_13$ with $x=0.034$, and an increase in x to 0.067 (Ref. 9) or 0.085 (Ref. 1) continuously worsens the reproduction of the intensity ratio of the (110) and (200) rings.

The top inset in Fig. 4 shows the present equation of state (EOS) data together with previously determined atomic volumes.[22,23] Fitting a Birch-Murnaghan equation with $B'=4$ to the cg-N data results in a zero pressure atomic volume of 6.69 Å^3 and a bulk modulus B_0 of 261 GPa. Mailhiot *et al.*[1] had predicted 6.67 Å^3 and a B_0 of 341 GPa, astonishingly close to the present data.

Based on present and previous[18,19,22–25] results, we propose a conceptual chemophysical phase diagram in Fig. 5, with emphasis on the molecular to nonmolecular phase transformation. The boundary (dot-dash line) is constructed based on the following facts: (i) all laser-heating experiments show that a transformation occurs above 110 GPa; (ii) the transformation pressure rapidly increases at temperatures lower than 500 K (Refs. 18 and 19); and (iii) theoretical calculations of the Grüneisen parameter $\gamma=V(\partial P/\partial E)_V$, based on previous shock-wave data,[24,26] give rise to a nearly vertical molecular-to-nonmolecular transformation line at temperatures above 2000 K and even deep into the liquid.

Note the strong curvature in the molecular/nonmolecular transformation boundary in Fig. 5, which signifies the strong kinetic effects associated with the transition at relatively low temperatures between 400 and 700 K. Therefore, the polymerization to cg-N at ambient temperature (blue arrow) is strongly delayed, if not limited, which may in turn provide an alternate route to an insulator-metal transition. The semiconducting nature of amorphous η-N is perhaps the state arising prior to such a band-gap closure. However, such kinetic issues are becoming less important at high temperatures, as indicated by the nearly vertical transition line. Thus, nitrogen polymerization is relatively more viable at high temperatures (red arrow), as the increase in entropy favors more dissociated states (i.e., less saturated nitrogen bonds).

Indeed, the formation of the reddish amorphous phase and then cg-N at high temperatures suggests a stepwise opening of the nitrogen-nitrogen triple bonds in ζ-N_2 to N═N and then to N—N. This transformation model may then be viewed as a concerted *SN*-2 type polymerization,[27] with the amorphous phase acting as an "intermediate" state. While the existence of such an intermediate state substantially lowers the threshold for the formation of an extended solid, understanding the stability and structure of amorphous nitrogen may be more challenging, both experimentally and theoretically, as it may represent one of many local energy minima existing on a complicated energy landscape.[28]

This work was performed under the auspices of the U.S. Department of Energy under Contract No. W-7405-ENG-48 at LLNL. The x-ray work was performed at beamline 16IDB of the HPCAT at the APS, supported by DOE-BES and DOE-NNSA (CDAC, LLNL, UNLV).

[1] C. Mailhiot, L. H. Yang, and A. K. McMahan, Phys. Rev. B **46**, 14419 (1992).
[2] R. Hoffmann, Angew. Chem., Int. Ed. Engl. **21**, 711 (1982).
[3] R. Boehler, Mater. Today **8**, 34 (2005).
[4] V. Iota, C. S. Yoo, and H. Cynn, Science **283**, 1510 (1999).
[5] M. J. Lipp, W. J. Evans, B. J. Baer, and C. S. Yoo, Nat. Mater. **4**, 211 (2005).
[6] R. J. Hemley, Annu. Rev. Phys. Chem. **51**, 763 (2000).
[7] E. Gregoryanz, A. F. Goncharov, R. J. Hemley, H.-K. Mao, M. Somayazulu, and G. Shen, Phys. Rev. B **66**, 224108 (2002).
[8] R. Bini, L. Ulivi, J. Kreutz, and H. J. Jodl, J. Chem. Phys. **112**, 8522 (2000).
[9] M. I. Eremets, A. G. Gavriliuk, I. A. Trojan, D. A. Dzivenko, and R. Boehler, Nat. Mater. **3**, 558 (2004).
[10] T. W. Barbee III, Phys. Rev. B **48**, 9327 (1993).
[11] K. O. Christe, W. W. Wilson, J. A. Sheehy, and J. A. Boatz, Angew. Chem., Int. Ed. **38**, 2002 (1999).
[12] C. S. Yoo, J. Akella, H. Cynn, and M. Nicol, Phys. Rev. B **56**, 140 (1997).
[13] E. Gregoryanz, C. Sanloup, M. Somayazulu, J. Badro, G. Fiquet, H.-K. Mao, and R. Hemley, Nat. Mater. **3**, 294 (2004).
[14] J. C. Crowhurst, A. F. Goncharov, B. Sadigh, C. L. Evans, P. G. Morrall, J. L. Ferreira, and A. J. Nelson, Science **311**, 1275 (2006).
[15] M. Popov, Phys. Lett. A **334**, 317 (2005).
[16] Y. Akahama and H. Kawamura, J. Appl. Phys. **96**, 3748 (2004).
[17] R. S. Hixson and J. N. Fritz, J. Appl. Phys. **71**, 1721 (1992).
[18] M. I. Eremets, R. J. Hemley, H.-K. Mao, and E. Gregoryanz, Nature (London) **411**, 170 (2001).
[19] E. Gregoryanz, A. F. Goncharov, R. J. Hemley, and H.-K. Mao, Phys. Rev. B **64**, 052103 (2001).
[20] A. F. Goncharov, E. Gregoryanz, H.-K. Mao, Z. Liu, and R. J. Hemley, Phys. Rev. Lett. **85**, 1262 (2000).
[21] G. Herzberg, *Electronic Spectra and Electronic Structure of Polyatomic Molecules* (van Nostrand, New York, 1966), 416 pp.
[22] H. Olijnyk, J. Chem. Phys. **93**, 8968 (1990).
[23] M. I. Eremets, A. G. Gavriliuk, N. R. Serebryanaya, I. A. Trojan, D. A. Dzivenko, R. Boehler, H.-K. Mao, and R. J. Hemley, J. Chem. Phys. **121**, 11296 (2004).
[24] M. Ross and F. Rogers, Phys. Rev. B **74**, 024103 (2006).
[25] A. S. Zinn and D. Schiferl, J. Chem. Phys. **87**, 1267 (1987).
[26] H. B. Radousky, W. J. Nellis, M. Ross, D. C. Hamilton, and A. C. Mitchell, Phys. Rev. Lett. **57**, 2419 (1986).
[27] H. Sasaki, J. M. Rudzinski, and T. Kakuchi, J. Polym. Sci. A **33**, 1807 (1995).
[28] W. D. Mattson, D. Sanchez-Portal, S. Chiesa, and R. M. Martin, Phys. Rev. Lett. **93**, 125501 (2004).